Eng.&Technology, Vol.25, No.3, 2007

On-Line Current-Based Condition Monitoring and Fault Diagnosis of Three-Phase Induction Motor

Prof.Dr. K. S. Krikor* **Ali H.Numan. M.Sc.****

Received on: 5/9/2005
Accepted on: 29/1/2006

Abstract:
A stator current measurement has an important role in condition monitoring and fault diagnosis of induction motors. For instance, the eccentricity, rotor bars and end ring breaks, shorted stator windings can be detected by analyses based on stator current measurement. This paper addresses the application of stator current spectral analysis technique for the detection and localization of abnormal electrical and mechanical conditions that indicate, or may lead to, a failure of the induction motors. The effects of stator current spectrum are described and the related frequencies are determined. In the present investigation, the frequency signatures of some asymmetrical motor faults are well-identified using signal processing techniques, such as Welch method for spectral density estimation. In fact, experimental results clearly illustrate that stator current spectral analysis using Welch method is a very good tool to detect faults in induction motors. These faults are shaft speed oscillation, eccentricity, broken rotor bar, and end ring cracked.

Keywords: Motor current signature analysis, on line, fault diagnosis, three-phase induction motor.

الخلاصة:
تعتبر طريقة فحص بصمة التيار من الطرق الدقيقة والتي لعبت دور كبيرفي تشخيص ومراقبة الاعطال في المحركات الحثية ومن تلك الاعطال التي يمكن كشفها عن طريق فحص بصمة التيار هو عدم الانتظام سواء كان في الجزء الساكن او الدوار والدوائر المفتوحة في قضبان الدوار وفي الحلقات الانهائية وكذلك الدوائر المقصورة في ملفات الجزء الساكن كل تلك الاعطال يمكن كشفها وتحديد موقعها بدقة من خلال فحص بصمة تيار الجزء الساكن.ان البحث الحالي يتناول موضوع تطبيق تحليل الطيف الترددي لبصمة التيار لكشف وتحديد بعض الاعطال الكهربائية والميكانيكية والتي يمكن ان تؤدي الى احداث خلل في عمل المحركات الحثية.لقد تم تحديد الترددات المرافقة لبعض الاعطال بشكل جيد من خلال تحليل الطيف الترددي للتيار عن طريق تقنيات معالجة الاشارة ومثال على احد تلك التقنيات طريقة ويلش لتخمين كثافة ومحتوى الطيف الترددي للتيار .لقد اثبت البحث الحالي ومن خلال التجارب العملية التي اجريت ان تحليل الطيف الترددي لتيار الجزء الساكن باستخدام طريقة ويلش كان دقيقاً جداً وناجحاً في تحديد وكشف الاعطال الناجمة عن تذبذب سرعة دوران الجزء الدوار وكذلك عدم الانتظام في الجزء الساكن او الدوار بالاضافة الى الدوائر المفتوحة في قضبان الجزء الدوار او في الحلقات الانهائية.

* Dept. of Technical Education, UOT., Baghdad-IRAQ.

I. Introduction

Companies dealing with electrical machinery find condition monitoring and diagnostics more and more important. The supervision of electrical drive systems using non-invasive condition monitoring techniques is becoming state of the art method for improving the reliability of electrical drives in many branches of the industry. Typical questions are, how to detect incipient faults, how to distinguish a deteriorating fault from a harmless constructional asymmetry, which are the physical quantities that best indicate a fault and how to measure them, and how should the measured signals be processed to get the most reliable diagnosis.

Recently, a Stator line current spectral analysis technique has been widely used for the purpose of condition monitoring and fault detection in induction motors. This current can be easily measured without interruption to the machine operation, and hence allows on-line fault detection [1]-[3]. Prodigious improvement in signal processing hardware and software has made this possible. Primarily, these techniques depend upon locating specific harmonic components in the line current, also known as motor current signature analysis (MCSA). These harmonic components are usually different for different types of faults. Furthermore, other signals such as speed, torque, noise, vibration etc., are also explored for their frequency contents. Sometimes, altogether different techniques such as thermal measurements, chemical analysis, etc., are also employed to find out the nature and the degree of the fault [4]-[6].

Different kinds of artificial intelligence based methods have become common in fault diagnostics and condition monitoring. For example fuzzy logic and neural networks (NN) have been used in modeling and decision making in diagnostics schemes. Also, numerical classification methods are widely used in area of modern fault diagnostics, and they are attracting a following also in fault diagnostics of electrical machines. For example, in [7] and [8], NN based classifiers are used in diagnosis of rolling element bearings.

There is an increasing demand for automated condition monitoring of motors performing critical tasks. Sudden breakdown and unscheduled maintenance of machines might often mean revenue loss and disruption of targeted production. Thus on-line condition monitoring and fault diagnosis is a very desirable feature. This paper investigates experimentally the feasibility of detecting faults in induction motors by performing motor current signature analysis (MCSA).

II-Motor Current Signature Analysis

There are various types of current spectra which contain fault information. These frequencies are derived from the physical construction of the machine:

1) Bearing Faults

The roller element bearing is one of the most crucial components in rotating electrical machinery. Rolling bearing generally consists of two rings which are called the outer raceway and the inner raceway with a set of rolling elements in their tracks.

When the bearing is not installed properly into the shaft or into the housing, its raceway can generate stator current harmonics with frequencies calculated by [9].

$$f_{bng} = \left| f_s \pm n_b f_{i,o} \right| \quad (1)$$

with,

$$f_{i,o} = \frac{n}{2} f_r [1 \pm \frac{BD}{PD} \cos b] \quad (2)$$

where n=1,2,3--- , n_b is the number of balls, fs the electrical supply frequency, $f_{i,o}$ the frequency of bearing inner and outer raceway, f_r the mechanical rotor speed in hertz, PD the bearing pitch diameter, BD the ball diameter, and β the contact angle of the ball on the races, as shown in Fig.1.

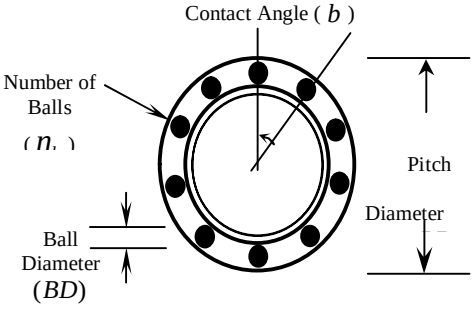

Fig.1 Ball bearing dimensions.

2) Broken Bars and Eccentricity Faults

The reasons for rotor bar breakage are several. Generally, broken bar may be distinguished from rotor asymmetry by examining the harmonics sidebands. If asymmetry is exist, an smooth variation of air-gap flux density will appear. It has been shown that both static and dynamic eccentricities will give rise to current harmonics at frequencies given by [9]

$$f_{ecc} = f_s \left[(nN_r \pm n_{ecc}) \left(\frac{1-S}{P} \right) \pm n_s \right] \quad (3)$$

where Nr is the rotor bars number, n_{ecc} the eccentricity order number, S the per unit slip, P number of pole pairs ,and ns the supply harmonic rank.

3) Shaft Speed Oscillation Faults

In case of dynamic eccentricity, the center of the rotor is not at the center of the rotation and the position of minimum air-gap rotates with the rotor. This oscillation will produce variations in the air-gap flux density. This, in turn, will affect the inductance of the electrical machine producing stator current harmonics with frequencies predicted by [9].

$$f_{sso} = f_s \left[k \left(\frac{1-S}{P} \right) \pm 1 \right] \quad (4)$$

where k is any integer.

4) Rotor Asymmetry Faults

Since the air-gap flux density is perturbed as has been shown in the preceding case, this perturbation will rotate at shaft speed. The frequencies of the spectral components in the air-gap flux density are given by [9].

$$f_{ra} = f_s \left[k \left(\frac{1-S}{P} \right) \pm 1 \right] \quad (5)$$

III. Description Of Experimental System

In this section, the elements of data acquisition system for stator current monitoring illustrated in Fig.2 will be present to perform experiments on three-phase induction motor under fault conditions.

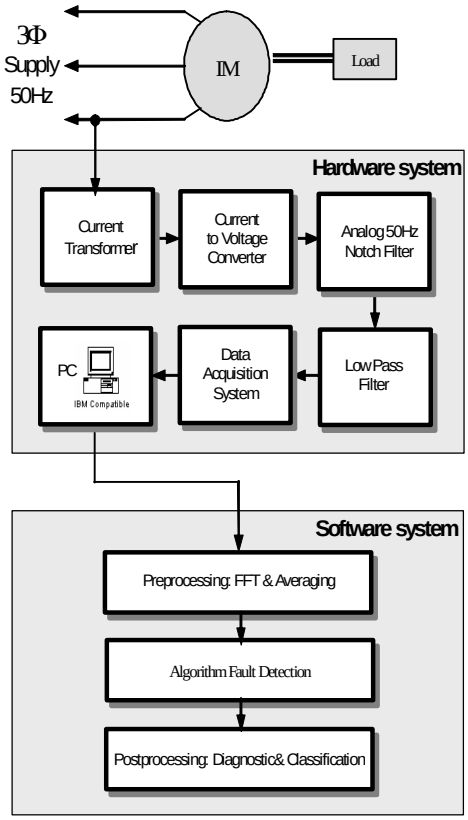

Fig.2 Block diagram of on-line stator current monitoring system.

A. Hardware System

a) Current Transformer (CT)

The current transformer of type (clamp-on) were used to reduce the magnitude of stator current.

b) Current to Voltage Converter(C/V)

Since all electronic components that was used in the design of system hardware is process only voltage signal, thus the current to voltage converter is used for this purpose, which consist of resistor 250 ohm shunted on the output of current transformer to produce voltage signal between 1 to $\pm$ 5 volts [10]. This level of voltage signal is very proper to all electronic components of the system hardware such as analog to digital converter (A/D).

c) Analog Notch Filter

The purpose of the notch filter is to filtering only the 50Hz without any other frequencies, thus reducing the fundamental components 50Hz of the signal.

d) Low Pass Filter

This filter has been used to remove higher frequency components of the stator current caused by Electromagnetic and Radio Frequency Interferences (EMI/RFI). The 4^{th} Chebyshev analog filter utilized for this purpose.

e) Data Acquisition System

The data acquisition system has been designed and implemented to measure motor current under software programs control and save the motor current samples at the hard disk drive of the personal computer (PC) through the motherboard industry standard architecture (ISA slot) to accomplish Fast Fourier Transform (FFT) and then display the results on the monitor of computer. The (AD574) have been used as Analog-to-Digital converter (A/D), which is a complete (12-bits) successive approximation analog-to-digital converter (A/D), with three output buffer circuitry for direct interface to a microprocessor. The conversion time is (15μsec), with (2.44 mv) resolution. The (A/D) converter samples the filtered current signal at(1kHz). The (MAX158) used to acquire data from the current sensors (MAX158 pin names A0 through A7). The photo in Fig.3 shows data acquisition system.

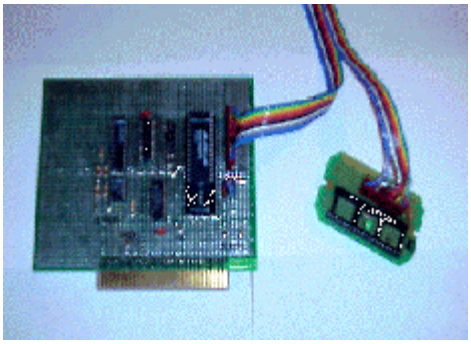

Fig.3 Data acquisition system.

Two types of the components selected for the data acquisition system, namely, the peripheral programmable interface (PPI), and the timers, are programmable and need to be configured before the card can start its operation. Moreover, the operation of the multiplexer and the (A/D) is controlled through software in order to select the channel to be sampled and the start and end of conversion. Also, since several parameter for the interface card can be set by the user through the personal computer (PC) keyboard, an interface program between the user and the card must be available. Finally, the software is written in C language in order to get high speed of processing in the personal computer (PC). Fig.4 shows the flow chart of data acquisition software program.

f) Personal Computer (PC)

The hardware and the software systems has been implemented using 500MHz Pentium (II) personal computer (PC). The purpose behind use of PC for its availability, processing speed and storage capability, this equipment can be efficiently used to perform miscellaneous measurements. However, the PC was performed two tasks, storage the data collected from the induction motor current and then displaying the processed data after applying the algorithm for extraction useful information regarding faults.

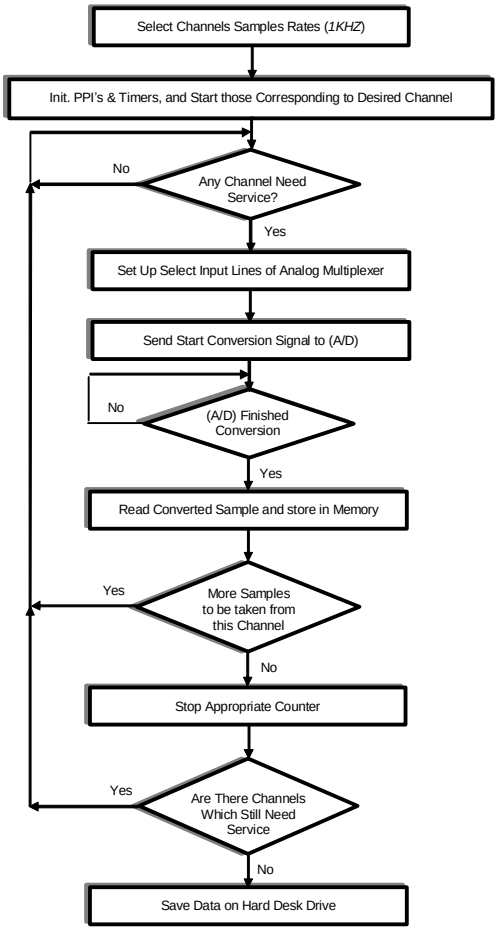

Fig.4 Flow chart of data acquisition software programs.

B.Software System

1) Signal Preprocessing (FFT& Averaging)

The signal used as a basis for condition monitoring as stated before is motor stator phase line current. The preprocessors convert the sampled signal to the frequency domain using Fast Fourier Transform (FFT) algorithm to generate the power spectral density (PSD). The PSD is one of the most useful signal

processing techniques, which has been the estimation of spectrum of discrete time deterministic and stochastic processes. This estimate is called the periodgram whose processes simply find the discrete-time Fourier transform of the collected signals take the squired magnitude of the results. The spectrum generated by this transformation includes only the magnitude information about the frequency component. Signal noise that is present in the calculated spectrum is reduced by averaging the predetermined sections (or windows) of a signal large sample set. Because of the frequency range of interest and the desired frequency resolution, the processing section generates several thousand-frequency components.Fig.5 shows steps to implement Welch's periodogram averaging technique [11].

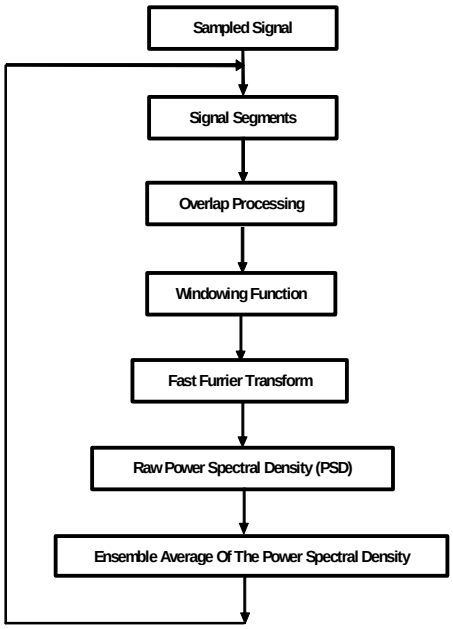

Fig. 5 Steps for estimating the power spectral density (PSD).

a) Signal Segment and Overlap Processing

As the number of samples increases, the expected value of the periodogram approaches the real PSD. In spite of the fact that the number of samples increases, the variance of the periodogram estimate does not decrease. One way of reducing the variance of the PSD estimate is to divide into more segments and average the periodograms of the segments. The more segment we average, the lower the statistical variance of the result. In order to obtain the more segments the overlap processing is used to overlap time records. When overlap rates are over half the segment length, they have been found to lower the variance of the estimate significantly .The signal X(n) is divided into (K) segments and let the (i^{th}) segment of X(n) be $S_i(n)$,(i=0,1,2,…,K),(n=0,1,2,…,M-1).When over lapping is employed, ($K \geq N/M$) and each segment length (M).

b) Windowing Function

A window is a time domain weighting function applied to the input signal. A window is a filter used to remove signals that is not periodic (and therefore spurious) within the input time record. This makes the input time record appear to be a periodic signal, usually by forcing the amplitude to zero at both ends of the time record. Selecting the proper window can prevent "leakage" a measuring of energy across the frequency spectrum caused by transforming signals that are not periodic within the time record. Applying a suitable proper data window (such as Hanning, Flat-top,

or Uniform) to the chosen segments can improve the periodogram estimate prior to computing the periodogram, resulting in a modified periodogram. The ith segment of data is then multiplied by a proper data window ω (n). This provides some control over the effects of spectral leakage .The windowing data is expressed as:

$$sw_i = w(n) \times ws_i(n) \quad (6)$$

where $\omega s_i(n)$ is time domain signals, and ω(n) suitable data window.

c) Fast Fourier Transform (FFT)

Within each segment, applying FFT (Fast Fourier Transform) can convert time domain signals $\omega s_i(n)$ into the frequency domain.

$$ws_i(f) = \frac{1}{M} \sum_{n=0}^{M-1} ws_i(n)\, e^{-j2\pi n \frac{f}{M}} \quad (7)$$

f=0,1,2,…N, where f is discrete frequency, the raw power spectral estimate can be formed:

$$PSD_i(f) = ws_i(f) \times ws_i^*(f) \quad (8)$$

where * denotes the complex conjugate. The ability to average a series of measurements is useful to discriminate between noise and components that are actually part of the signal. This ensemble-averaging technique is very effective for determining the frequency content of a signal buried in a random noise. The raw PSD estimates from all (K) segments can then be averaged to give the following estimates:

$$PSD(f) = \frac{1}{k} \sum_{i=0}^{k-1} PSD_i(f) \quad (9)$$

2) Fault Detection Algorithm

In order to reduce the large amount of spectral information to a usable level, an algorithm, in fact, a frequency filter eliminates those components that provide no useful failure information. The algorithm keeps only those components that are of particular interest because they specify characteristic frequencies in the current spectrum that are known to be coupled to particular motor faults. Since the slip is not constant during normal operation, some of these components are bands in the spectrum where the width is determined by the maximum variation in the slip of motor.

3) Postprocessing

Since a fault is not a spurious event, but continues to degrade the motor, the postprocessor diagnoses the frequency components and then classifies them (for each specified fault).

IV. Experimental Results

To verify the generality of the presented considerations. Laboratory experiments were performed on a thee phase squirrel cage induction motor, the motor parameters are depicted in appendix (I). The investigated drive system is shown in Fig.6.

Fig.6 Experimental test-bed.

Experiment (1):Healthy motor

In this experiment, the motor is fed by three phase balance supply where the drive system driving the full load at 1444 r.p.m .The stator power spectra of Fig. 7 represents then, in our case, the supposed healthy motor. From Fig.7 it is clear that the amplitude of the fundamental stator current frequency 50Hz as expected, is the largest one from all other harmonics of stator current. Since the supply voltage is three phase without neutral connection, thus in the healthy case the third harmonic and its multiple will not be appear in the stator current power spectra. The amplitude of the fifth harmonic is less than that of the fundamental harmonic but it is greater than that of the seventh harmonics and so on.

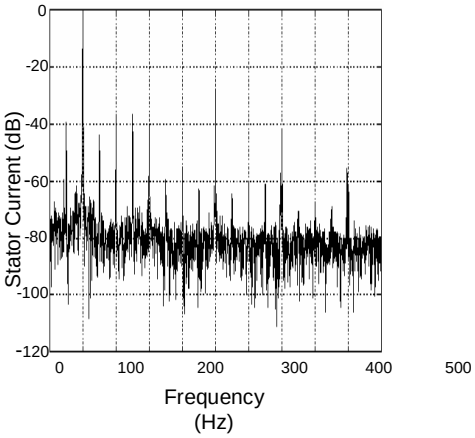

Fig.7 Full-load motor stator current spectra for healthy case.

Experiment (2): Faulty motor (broken rotor bar)

The motor is run under full load as in the preceding experiment, but this time when multiple of its rotor bars is breakage. The broken bar is created through drilling the bar from the connection region with end ring segment and that is mean one rotor loop with its current is removed. Fig. 8 shows stator current power spectra when the motor driving the full load at 1444(r.p.m) with one broken rotor.

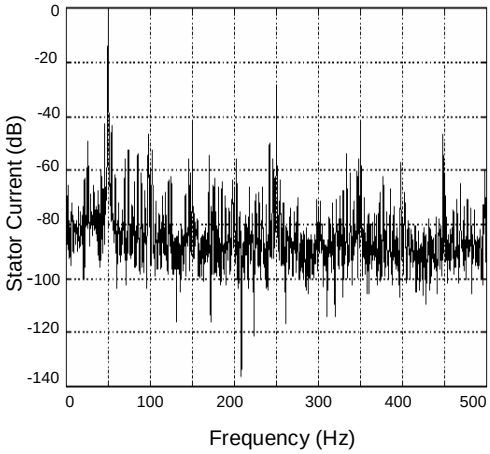

Fig. 8 Full-load motor stator current spectra with one broken rotor bar.

However, since the motor stator current is quite noisy (distorted), that makes it difficult to correctly distinguish between healthy and faulty conditions by depending only upon the operator skills. Thus, when zooming the power spectra of stator current of Fig. 8 more information appears as shown in Fig.9 that makes the errors in decision which make the operator decide that case is healthy or not, this is more accurate than that of the previous one.

From Fig.9 and according to equation (3), it can be seen the side band harmonics which is equal in our case to (46Hz for low side and 54Hz for upper side harmonics) and the amplitude of these two side band harmonics increase in significant way with increase number of broken bar. By monitoring the amplitude of the side band harmonics it gives good warring for incipient broken rotor bars and end ring cracks. However,

sometimes these two side band harmonics appears even if the motor is not faulty due to uneven rotor bar resistance resulting in manufacturing process such as die casting process or rotor bar asymmetry etc. as will be shown in the next experiment.

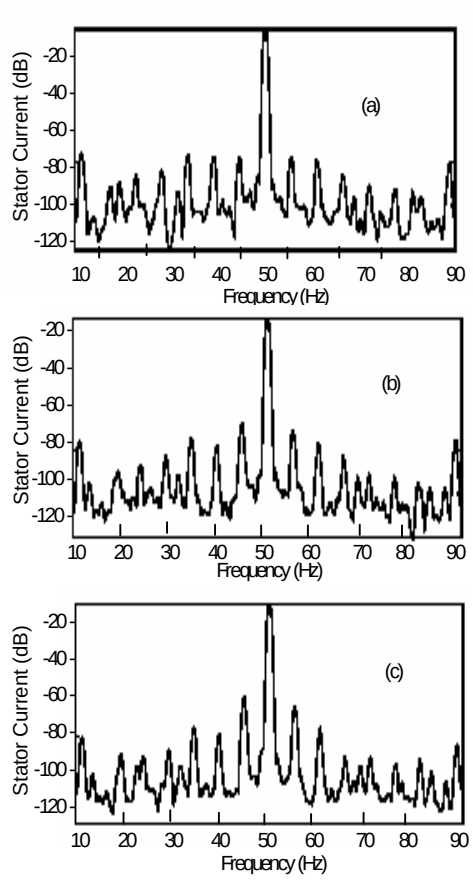

Fig. 9 Stator current power spectra around 50Hz with one,(b)two ,and (c) three adjacent broken bars.

Experiment (3):Faulty motor (eccentric rotor)

The motor has been loaded with disc. The disc was drilled with four small holes on the corner of it to emulate the rotor dynamic eccentricity. According to equation (3) the eccentricity harmonics (26 and 74Hz) will appear in the stator line current power spectra as shown in Fig.10.

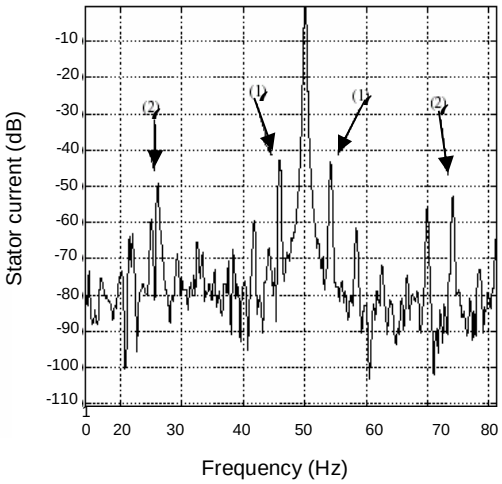

Fig. 10 Stator current power spectra around 50Hz.

In addition to these harmonics there is also side band harmonics appear in the same figure, but this time no broken rotor bar has been occur in the cage of the motor. However, these side band harmonics appears in the case of healthy motor due to the previous mentioned reasons in the preceding experiment. The shaft speed oscillation occurs in the case of dynamic eccentricity that varies with rotor position, the oscillation in the air-gap length causes variations in the air-gap flux density. This in turn affects the inductance of the machine producing stator current harmonics with frequencies, see equation (3). In Fig.11 the shaft speed oscillation appears clear at a 246 Hz.

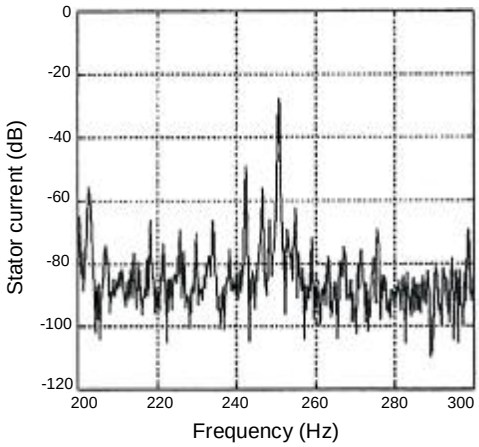

Fig.11 Stator current power spectra for frequencies more than 200Hz.

Experiment (4):Faulty motor (unbalance supply)

In this experiment, the stator voltages were unbalanced by adding a resistance to one phase of the stator. The value of this resistance has been chosen to be 0.2 p.u. , and the resistance is connected in series with phase (A) of motor, and thus the voltage drop across this resistance is responsible of reduced the applied voltage to phase (A) that in turn causes stator voltage to be unbalanced. The experimental result is depicted in Fig.12. One should notice the emergence of even harmonics, where the appearance of even harmonics (2th, 4th,6th and so on) is the indication of an unbalance in the operation of the motor which causes the motor to draw a negative phase sequence current.

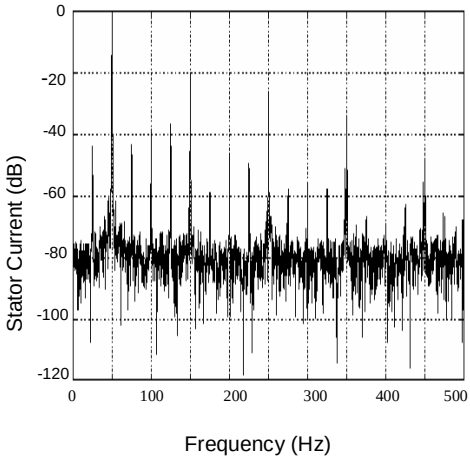

Fig.12 Stator current power spectra in the case of stator voltage unbalance**.**

Experiment (5):Faulty motor (open phase)

The last experiment dealt with the analysis of a single- phase effect corresponding to a stator open phase, were phase (A) of the motor is opened and the rest of two phases (B&C) are connected to three phase supply. The experimental result of this case is depicted in Fig.13 which illustrates in this case the power spectra of the stator current. As with the previous remark, we notice the emergence of even harmonics, but with less amplitude.

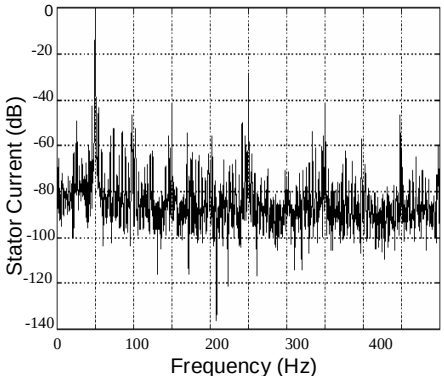

Fig. 13 Stator current power spectra in the case of open phase.

V. Conclusions

In this paper, the effectiveness and feasibility of non-invasive motor current signature analysis (MCSA) for fault diagnosis of three phase squirrel cage induction motor has been explored. The effects of stator current spectrum have been described and the related frequencies determined. In the present investigation, the frequency signatures of some asymmetrical motor faults have been well identified using Welsh method for power spectrum estimation technique. Extensive corroborative experimental studies are necessary to full assess usefulness of the proposed technique for the preventive maintenance diagnostics and failure prevention in drive system with induction motors.

APPENDIX (I)

The induction motor that is used in the experimental tests of this paper is a Siemens with the following data:

Motor Parameter		Unit
1	Output power (P)	4KW
2	Rated voltage (Y/Δ)	(380/220) v
3	Rated current (Y/Δ)	(7.8/15.3) A
4	Number pole pairs (P)	٢
5	Supply frequency (f)	50Hz
6	Synchronous speed(Ns)	1500 (r.p.m)
7	Rated rotor speed (Nr)	1444(r.p.m)
8	Stator Resistance (Rs)	1.6 Ω
9	Stator Leakage Inductance (Ls)	0.25 H
10	Rotor Bar Resistance (Rb)	42.11 μΩ
11	Rotor Bar leakage Inductance (Lb)	0.8 μH
12	Rotor End Ring Leakage inductance (Le)	0.02 μH

References

[1] Kliman G. B. and Stein J.,"Induction motor fault detection via passive current monitoring", *International Conference in Electrical Machines*, Cambridge, MA, pp.13-17, August 1990.

[2] Kliman G. B. and Stein J., "Methods of motor current signature analysis", *Elec.Mach.Power Syst.*vol.20, pp.463-474, Sep.1992.

[3] Kliman G. B., Premerlani W. J., R. Koegl A. and Hoeweler D., " A new approach to on-line fault detection in ac motors", *IEEE-IAS Annual Meeting Conference*, pp.687-693, San Diego, CA, 1996.

[4] Dorrell D. G., Thomson W. T. and Roach S., "Analysis of airgap flux, current, vibration signals as a function of the combination of static and dynamic airgap eccentricity in 3-phase induction motors", *IEEE Trans. Ind. Applns.*, vol. 33, no.1, pp. 24-34, 1997.

[5] Said M.S.N., and Benbouzid M.E.H. "H-G diagram based rotor parameter identification for

induction motors thermal monitoring ”*IEEE Trans. on Energy Conv.*, vol.15, no.1, pp.14-18, Mar. 2000.

[6] Mirafzal B. and Demerdash N. A. O., “On innovative methods of induction motor inter-turn and broken-bar fault diagnostics” *in Conf. Rec. Proc. IEEE-IEMDC 2005*, May 15-18, 2005.

[7] Penman J., and Yin C.M., “Feasibility of using unsupervised learning, artificial neural networks for the condition monitoring of electrical machines”, *IEE Proceedings on Electr. Power Applns.*, pp. 317-322, vol. 141, no.6, Nov.1994.

[8] Kim K., Parlos A.G, “Induction motor fault diagnosis based on neuropredictors and wavelet signal processing”, IEEE Transactions on Mechatronics vol.7, no.2, pp.201-219, Jun 2002.

[9] Vas P., Parameter estimation, condition monitoring, and diagnosis of electrical machines, Clarendron Press, Oxford, 1993.

[10] Zbigniew Krajewski, New horizons in data acquisition and computer interfaces, Omega Press LCC, 1997.

[11] Vaseghi S.V., Advanced digital signal processing and noise reduction, John Willy & Sons, Ltd, 2000.